MOLECULAR ELECTRONICS AND HYBRID COMPUTERS

Molecular electronics is an interdisciplinary field which lies at the interface of chemistry, electrical engineering, optical engineering, and solid-state science. It is defined as the en-

J. Webster (ed.), *Wiley Encyclopedia of Electrical and Electronics Engineering*.

Table 1. Characteristics, Potential Advantages and Current Disadvantages of Implementing Molecular Electronics

Characteristic	Potential Advantages	Current Disadvantages
Size/speed	Small size of molecular scale offers high intrinsic speed. Picosecond switching rates are common.	Small size makes connection to control, input and output circuitry difficult.
Architecture	Neural, associative and parallel architectures can be implemented directly.	Three-terminal devices and standard logic designs are difficult to implement.
Quantized behavior	The quantum mechanical properties can be engineered with high precision.	Quantized behavior limits electron current densities and architectural flexibility.
Nanoscale engineering	Synthetic organic chemistry, self-assembly and genetic engineering provide nanometer resolution.	Nanolithography provides higher scale factors and flexibility than current molecular techniques.
Stability	Some molecules and proteins offer thermal and photochemical stabilities comparable to bulk semiconductors.	Most molecules and proteins are photochemically or thermally labile, precluding general application.
Nonlinear properties	Intrinsic second- and third-order properties of molecules can be synthetically optimized.	Lifetimes and damage thresholds of molecular based nonlinear optical devices are not yet competitive.
Reliability	Ensemble averaging using optical coupling or state assignment averaging provides high reliability.	Thermal or photochemical stress, impurity effects, and quantum statistics limit reliability of many systems.

coding, manipulation, and retrieval of information at a molecular or macromolecular level. This approach contrasts with current commercial techniques, which are exponentially approaching their practical (economic) limits, and where these tasks are accomplished by lithographic manipulation of bulk materials to generate integrated circuits. Molecular electronics not only represents the final technological stage in the miniaturization of computer circuitry, but it also promises new methods for high-speed signal processing and communication, volumetric data storage, novel associative and neural architectures, as well as linear and nonlinear devices and memories. The ability to explore new architectures unique to molecular based systems has a potential equal to that provided by molecular-scale engineering and miniaturization.

Biomolecular electronics (bioelectronics) is a subfield of molecular electronics that investigates the use of native as well as modified biological molecules (chromophores, proteins, etc.) in place of the organic molecules synthesized in the laboratory. Because natural selection processes have often solved problems of a similar nature to those that must be solved in harnessing organic compounds, and because self-assembly and genetic engineering provide sophisticated control and manipulation of large molecules, biomolecular electronics has shown considerable promise. It is commonplace to use the adjective "molecular" to cover both synthetic and natural sources of organic compounds.

ADVANTAGES AND DISADVANTAGES OF MOLECULAR BASED DEVICES

A majority of readers of this encyclopedia will have limited experience with molecular electronics. One of the best ways to introduce this field is to examine the potential advantages and disadvantages as outlined in Table 1. The list presented in Table 1 is neither exhaustive nor orthogonal. First, many additional characteristics could have been included. Those listed in Table 1 are selected to provide the broadest coverage with a minimum number of categories. Second, the characteristics are in some cases overlapping. For example, the reliability of a device is a function of the size and stability of the component molecules, the speed of the device, and the quantum mechanical properties of the molecule or molecular ensemble. Nevertheless, the characteristics listed in the first column of Table 1 represent the principal challenges to scientists seeking to implement molecular electronics. Each is discussed separately below.

Size and Speed

Molecules are synthesized from the "bottom up" by carrying out additive synthesis that starts with readily available organic compounds. Bulk semiconductor devices are generated "from the top down" by lithographic manipulation of bulk materials. A synthetic chemist can selectively add an oxygen atom to a chromophore with a precision that is far greater than a comparable oxidation step using electron beam or x-ray lithography. Molecular based gates are typically $\frac{1}{1000}$ the size of their semiconductor equivalents. At the same time, such gates have yet to approach a comparable level of reliability or interconnect capability as compared with their semiconductor counterparts.

The signal propagation times of molecular gates are due mainly to their small sizes. Whether the gate is designed to operate using electron transfer, electron tunneling, or conformational photochromism, a decrease in size will yield a comparable increase in speed. This is because all gates in use, under study, or envisioned are activated by the shift in the position of a charge carrier, and all charge carriers have mass. Whether the device is classical or relativistic, the mass of the carrier places a limit on how rapidly the conformational change can take place. Thus, size and speed are intimately related. One can criticize this view as arbitrarily restrictive in that electrostatic changes can be generated using optical excitation, and the generation of an excited electronic state can occur within a large chromophore in less than one femtosecond (one femtosecond = 10^{-15} s, the time it takes light to travel $\sim$0.3 μm). Nevertheless, the reaction of the system to the charge shift is still a size-dependent property, and the relationship between the total size of the device and the response time remains valid. A comparison of switching speeds of molecular gates versus those of some of the higher-speed semiconductor gates and switches is presented in Fig. 1.

The ultimate speed of a device is determined by other factors as well. Heisenberg uncertainty limits the maximum fre-

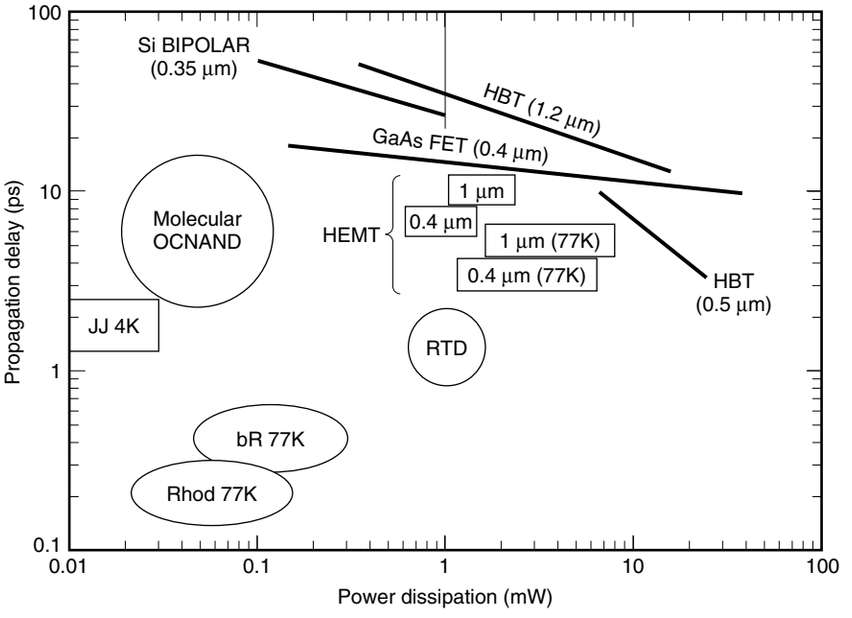

Figure 1. The propagation delay and power dissipation of selected molecular systems and semiconductor devices. The following abbreviations are used: HBT, hetero-junction bipolar transistor; HEMT, high electron-mobility transistor; RTD, resonant tunneling device; OCNAND, optically coupled NAND gate: JJ, Josephson junction; bR, bacteriorhodopsin primary photochemical event; Rhod, visual rhodopsin primary photochemical event. Feature sizes of the semiconductor devices are indicated in parentheses. Propagation delay of photonic molecular devices are defined in terms of the time necessary for the absorption spectrum to reach $1/e$ of the final photoproduct absorption maximum.

quency of operation, f_{max}, of a monoelectronic or monomolecular device, based on the following relationship (1):

$$f_{\max} \cong \frac{0.00800801 \cdot \tilde{v}_s \cdot \pi^2}{hN\left[2\pi + 2\tan^{-1}(-2) + \ln\left(\frac{\tilde{v}_s^2}{4}\right) - \ln\left(\frac{5\tilde{v}_s^2}{4}\right)\right]} \tag{1a}$$

$$f_{\max}(GHz) \approx \frac{0.963\tilde{v}_s}{N} \tag{1b}$$

where $\tilde{v}_s$ is the energy separation of the two states of the device in wavenumbers and N is the number of state assignments that must be averaged to achieve reliable state assignment. This equation only applies to monoelectronic or monomolecular devices; Heisenberg's uncertainty principle permits higher frequencies for ensemble averaged devices. For example, if a device requires 1000 state assignment averages to achieve reliability and $\tilde{v}_s \cong 1000$ cm^{-1}, it will have a maximum operating frequency of ~960 MHz. The concept of state assignment averaging is defined and quantitatively examined in Ref. 1. Virtually all monomolecular or monoelectronic devices require $N > 500$ at ambient temperature, but cryogenic devices operating at 1.2 K can approach $N = 1$. Thus, while molecular devices have an inherent advantage with respect to speed, quantum mechanics places constraints on the maximum operating frequency and these constraints are significant at ambient temperatures.

It is interesting to examine the trends in bit size that have characterized the last few decades of memory development. The results are shown in Fig. 2 and indicate that the area per bit has decreased logarithmically since the early 1970s (2,3). For comparison we also show in Fig. 2 the cross-sectional area per bit calculated for the human brain (assuming one neuron is equivalent to one bit), for proposed 3-dimensional memories, and proposed molecular memories. Although current technology has surpassed the cross-sectional density of the human brain, the major advantage of the neural system of

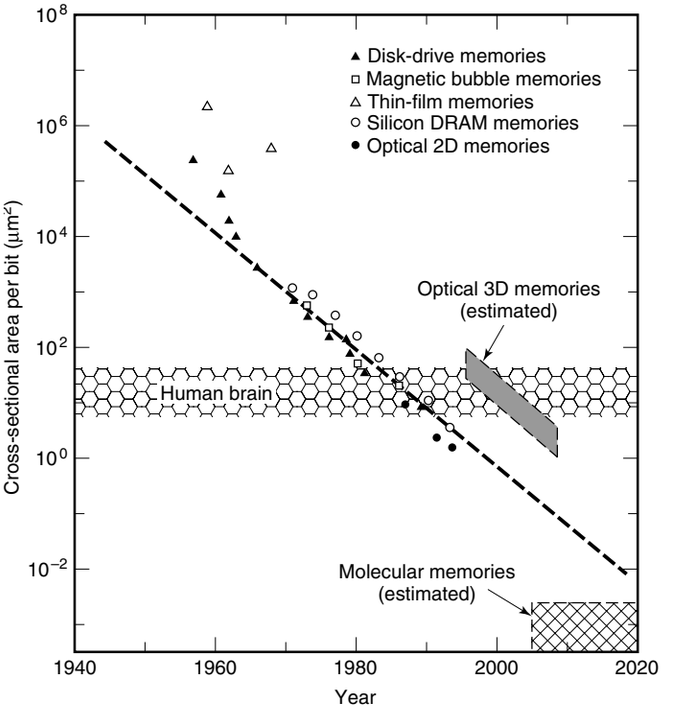

Figure 2. Analysis of the area in square microns required to store a single bit of information as a function of the evolution of computer technology in years. The data for magnetic disk, magnetic bubble, thin-film, and silicon DRAM memories are taken from Ref. 2. These data are compared to the cross-sectional area per bit (neuron) for the human brain, as well as anticipated areas and implementation times for optical 3-dimensional memories and molecular memories (3). Note that the optical 3-D memory, the brain, and the molecular memories are 3-dimensional, and therefore the cross-sectional area (A) per bit is plotted for comparison. The area is calculated in terms of the volume per bit, V/bit, by the formula $A = (V)^{2/3}$.

the brain is that information is stored in three dimensions. At present, the mind of a human being can store more "information" than the disk storage allocated to the largest supercomputer. Of course, the human brain is not digital, and such comparisons are tenuous. Nevertheless, the analogy underscores the fact that the current memory technology is still anemic compared to the technology that is inherent in the human brain. It also demonstrates the rationale for, and potential of, the development of 3-dimensional memories. We can also include from an analysis of Fig. 2 that the trend in memory densities will soon force the bulk semiconductor industry to address some of the same issues that confront scientists who seek to implement molecular electronics.

Architecture

Molecular electronics offers significant potential for exploring new architectures and represents one of the key features prompting the enthusiasm of researchers. This enthusiasm is somewhat tempered, however, by the recognition that the 3-terminal transistor that represents the fundamental building block of current computer gates and signal processing circuitry is difficult to implement using molecules. This problem, which also applies to Josephson junction devices, has either of two potential consequences. It could limit the role that molecular electronics will play in enhancing current computer and signal processing systems. Alternatively, it could encourage the investigation and development of new designs based on neural, associative, or parallel architectures and lead to hybrid systems with enhanced capabilities relative to current technology. This author considers the latter alternative to be far more likely. For example, optical associative memories and 3-dimensional memories can be implemented with unique capabilities based on molecular electronics (4). Implementation of these memories within hybrid systems is anticipated to have near-term application (see the section on Hybrid Computing). Furthermore, the human brain, a computer with capabilities that far exceed the most advanced supercomputer, is a prime example of the potential of molecular electronics (5). While the development of an artificial neural computer is beyond our current technology, it would be illogical to assume that such an accomplishment is impossible. Thus, we should view molecular electronics as opening new architectural opportunities that will lead to advances in computer and signal processing systems.

Quantized Behavior

Bandgap engineering and nanofabrication techniques have made possible a new class of quantum devices with unique functionalities (6). Quantum devices have the potential for greatly reducing the complexity of circuits, while simultaneously increasing the maximum frequency of operation. The fact that scientists and engineers working on bulk semiconductor gates have endorsed the potential of quantum devices is an indirect endorsement of molecular electronics. This position follows from a recognition that the quantum mechanical properties of molecules can be optimized for particular applications with considerable precision and growing sophistication. Quantized behavior is not always advantageous, however. Molecules invariably respond to the addition or subtraction of an electron with reorganization of the core electrons and the movement of the atoms in response to bonding changes. This characteristic limits the electron current a molecule can carry and complicates the design of 3-terminal devices that provide amplification. Thus, quantized behavior can limit architectural flexibility.

Nanoscale Engineering

The feature size of high-speed semiconductor devices has decreased dramatically during the evolution of computer technology (see Fig. 2). Driven by the demand for higher speeds and densities, micron and even submicron feature sizes are now commonplace. Ultraviolet lithography can provide modest improvement over current densities, but the evolution towards nanoscale feature sizes will require electron beam or X-ray lithography. While such lithography is well understood. it is very expensive to implement. As we have noted above, organic synthesis provides a "bottom up" approach that offers a 100- to 1000-fold improvement in resolution relative to the best lithographic methods. Organic synthesis has been developed to a high level of sophistication largely because of the efforts of natural product synthetic chemists to recreate a priori the complex molecules that nature has developed through billions of years of natural selection. There is already a sophisticated synthetic effort within the drug industry, and thus a commercially viable molecular electronic device could possibly be generated in large quantities using present commercial facilities.

There are two alternatives to organic synthesis that have had a significant effect on current efforts in molecular electronics, self-assembly, and genetic engineering. The use of the Langmuir-Blodgett technique to prepare organized structures is the best known example of self-assembly (7,8). However, self-assembly can also be used in the generation of membrane based devices, microtubule based devices, and liquid-crystal holographic films (7,8). Genetic engineering offers a unique approach to the generation and manipulation of large biological molecules. We discuss this unique element of bioelectronics below.

Thus, molecular electronics provides at least three discrete methods of generating nanoscale devices: organic synthesis, self-assembly, and site directed mutagenesis. That the latter two methods currently offer access to larger and often more complicated structures has been the reason for the early success of biomolecular electronics. All three techniques offer resolutions significantly better than those possible with bulk lithography.

High resolution is not the only criterion in examining the quality of nanoscale engineering. Lithography offers an advantage that none of the techniques available to molecular electronics can duplicate. Lithography can be used to construct very large scale integrated (VLSI) devices involving from 10^5 to 10^6 discrete components with complex interconnections. This ability can be quantitatively analyzed by defining the scale factor, a ratio defined as the overall area of the device divided by the size of the discrete gates or transistors that make up the device. A typical VLSI circuit has a scale factor of approximately 10^5. Despite the fact that organic synthesis offers convenient access to a 3-dimensional structure, the preparation of extremely large molecules is a significant challenge. A comparable scale factor for large organic molecules is approximately 10^3 to 10^4. Genetic engineering provides access to much larger structures, and scale factors

of 10^5 and even 10^6 are common. Nevertheless, the use of amino acid building blocks limits flexibility. Self-assembly expands the size still further, but at present the scale factors are small due to the use of identical molecules. In conclusion, nanoscale semiconductor engineering still provides the best combination of scale factor and flexibility.

Stability

One of the commonly claimed advantages of bulk semiconductor materials over organic molecules is thermal stability. Silicon and gallium arsenide can operate at temperatures that exceed those that most molecules can withstand for extended periods. However, many molecules and proteins can operate at very high temperatures and some have thermal stabilities that exceed those of silicon and gallium arsenide. Furthermore, the use of *ensemble averaging,* in which many molecules are used to simultaneously represent a single bit of information, enhances system stability by allowing some molecules to decompose without adversely affecting system reliability. Similar observations apply to photochemical stability, an issue relevant to optical computing and optical memories. For example, the protein bacteriorhodopsin, which is the light-transducing protein in the salt marsh bacterium *Halobacterium halobium,* exhibits outstanding thermal and photochemical stability (see the section entitled *Bioelectronics*). This is due in part to natural selection and in vivo requirement that this protein operate within a bacterium inhabiting a hot salt marsh under intense solar radiation. In summary, thermal and photochemical stability is an important issue in implementing molecular electronics, but organic and biological molecules can be designed with stabilities more than adequate for device applications.

Nonlinear Properties

There are many optical and electronic devices that make use of the nonlinear properties of the constituent materials. Most of the recent work in this area has concentrated on nonlinear optical properties because of the importance of these properties to the design of optical communication systems, optical computing, and optical memories. One of the principal advantages of using organic molecules in nonlinear optical applications is the ability to tailor the properties of the molecules to suit specific applications. Synthetic organic chemistry offers a level of flexibility in optimizing the dipole moment, transition moments, electronic symmetry, and conjugation length of a candidate material that exceeds the limitations inherent in manipulation of bulk inorganic materials. The principle problems encountered with present day nonlinear optical molecular materials are associated with transparency, damage threshold, and lifetime. Thus, while organic materials have been prepared with second-order hyperpolarizabilities much higher than lithium niobate, the latter inorganic material has found greater commercial application in second-harmonic generation. Organic materials, however, are rapidly closing the gap, and commercial viability is fast approaching (7,8).

Reliability

The issue of reliability has been invoked repeatedly by semiconductor scientists and engineers as a reason to view molecular electronics as impractical. Some believe that the need to use ensemble averaging in optically coupled molecular gates and switches is symptomatic of the inherent unreliability of molecular electronic devices. This point of view is comparable to suggesting that transistors are inherently unreliable because more than one charge carrier must be used to provide satisfactory performance. The majority of ambient temperature molecular and bulk semiconductor devices use more than one molecule or charge carrier to represent a bit for two reasons: (1) ensemble averaging improves reliability, and (2) ensemble averaging permits higher speeds. The nominal use of ensemble averaging does not, however, rule out reliable monomolecular or monoelectronic devices.

The probability of correctly assigning the state of a single molecule, p_1, is never exactly unity. This less than perfect assignment capability is due to quantum effects as well as inherent limitations in the state assignment process. The probability of an error in state assignment, P_{error}, is a function of p_1 and the number of molecules, n, within the ensemble used to represent a single bit of information. P_{error} can be approximated by the following formula (1):

$$P_{\text{error}}(n, p_1) \cong -\text{erf}\left[\frac{(2p_1+1)\sqrt{n}}{4\sqrt{2p_1(1-p_1)}} \cdot \frac{(2p_1-1)\sqrt{n}}{4\sqrt{2p_1(1-p_1)}}\right] \quad (2)$$

where erf $[Z_0; Z_1]$ is the differential error function defined by:

$$\text{erf}[Z_0; Z_1] = Erf[Z_1] - Erf[Z_0] \quad (3)$$

where

$$\text{erf}[Z] = \frac{2}{(\pi)^{1/2}} \int_0^Z \exp(-t^2)\, dt \quad (4)$$

Equation (2) is approximate and neglects error associated with the probability that the number of molecules in the correct conformation can stray from their expectation values based on statistical considerations. Nevertheless, it is sufficient to demonstrate the issue of reliability and ensemble size. First, we define a logarithmic reliability parameter, ξ, which is related to the probability of error in the measurement of the state of the ensemble (device) by the function, $P_{\text{error}} = 10^{-\xi}$. A value of $\xi = 10$ is considered a minimal requirement for reliability in nonerror-correcting digital architectures.

If we assume that the single molecule can be assigned correctly with a probability of 90% ($p_1 = 0.9$), then Eq. (2) indicates that 95 molecules must collectively represent a single bit to yield $\xi > 10$ [P_{error} (95, 0.9) $\cong 8 \times 10^{-11}$]. We must recognize that a value of $p_1 = 0.9$ is larger than is normally observed, and some examples of reliability analyses for specific molecular based devices are given in Ref. 1. In general, ensembles larger than 10^3 are required for reliability unless fault-tolerant or fault-correcting architectures can be implemented.

The question then arises whether or not we can design a reliable computer or memory that uses a single molecule to represent a bit of information. The answer is yes, provided one of two conditions apply: The first condition is architectural. It is possible to design fault-tolerant architectures which either recover from digital errors or simply operate reliably with occasional error due to analog or analog-type environments. An example of digital error correction is the use

of additional bits beyond the number required to represent a number. This approach is common in semiconductor memories, and under most implementations these additional bits provide for single-bit error correction and multiple-bit error detection. Such architectures lower the required value of ξ to values less than 4. An example of analog error tolerance is embodied in many optical computer designs that use holographic and/or Fourier architectures to carry out complex functions.

The second condition is more subtle. It is possible to design molecular architectures that can undergo a state reading process that does not disturb the state of the molecule. For example, an electrostatic switch could be designed which can be "read" without changing the state of the switch. Alternatively, an optically coupled device can be read by using a wavelength that is absorbed or diffracted, but that does not initiate state conversion. Under these conditions, the variable n, which appears in Eq. (1), can be defined as the number of read "operations" rather than the ensemble size. Thus our previous example, which indicated that 95 molecules must be included in the ensemble to achieve reliability, can be restated as follows: a single molecule can be used, provided we can carry out 95 nondestructive measurements to define the state. Multiple measurements are equivalent to integrated measurements, and should not be interpreted as a start-read-stop cycle repeated n number of times. A continuous read with digital or analog averaging can achieve the same level of reliability.

BIOELECTRONICS

There are many different bioelectronic devices that could be discussed here, but we will concentrate on one approach that has achieved recent success because of a major international effort involving research groups in the U.S., Canada, Europe, and Japan. The interest dates back to the early 1970s and the discovery of a bacterial protein that has unique photophysical properties. The protein is called bacteriorhodopsin and it is grown by a salt-loving bacterium that populates salt marshes. A light-absorbing group (called the chromophore) imbedded inside the protein matrix converts the light energy into a complex series of molecular events that store energy. Scientists using the protein for bioelectronic devices exploit the fact that the protein cycles through a series of spectrally distinct intermediates upon absorption of light. This complex series of thermal reactions results in dramatic changes in the optical and electronic properties of the protein. The excellent holographic properties of the protein derive from the large change in refractive index that occurs following light activation. Furthermore, bacteriorhodopsin converts light into a refractive index change with remarkable efficiency (approximately 65%). The size of the protein is one-tenth the wavelength of light (~500 nm light), which means that the resolution of the thin film is determined by the diffraction limit of the optical geometry rather than the "graininess" of the film. Also, the protein can absorb two photons simultaneously with an efficiency that far exceeds other materials. This latter capability allows the use of the protein to store information in three dimensions by using two-photon architectures. Finally, the protein was designed by nature to function under conditions of high temperature and intense light, a necessary requirement for a salt marsh bacterial protein and a significant advantage for photonic device applications.

Photonic Properties of Bacteriorhodopsin

When the protein absorbs light in the native organism, it undergoes a complex photocycle that generates intermediates with absorption maxima spanning the entire visible region of the spectrum (Fig. 3). Most current devices operate at ambient temperature and utilize the following two states: the initial green-red absorbing state (**bR**) and the long-lived blue absorbing state (**M**). The forward reaction only takes place by light activation and is complete in ~50 μs. In contrast, the reverse reaction can be either light activated or can occur thermally. The light activated $\mathbf{M} \rightarrow \mathbf{bR}$ transition is a direct photochemical transformation. The thermal $\mathbf{M} \rightarrow \mathbf{bR}$ transition is highly sensitive to temperature, environment, genetic modification, and chromophore substitution. This sensitivity is exploited in many optical devices that use bacteriorhodopsin. Another reaction of importance is a photochemical branching reaction from the **O** intermediate to form **P**. This intermediate form subsequently decays to form **Q**, a species that is unique in that the chromophore breaks the bond with the protein but is trapped inside the binding site. The **Q** intermediate is stable for extended periods of time (many years) but can be photochemically converted back to **bR**. This branching reaction provides for long term data storage as discussed later (9).

Associative Memories

Associative memories take an input data block (or image), and independently of the central processor, "scan" the entire memory for the data block that matches the input. In some implementations, the memory will find the closest match if it cannot find a perfect match. Finally, the memory will return the data block in memory that satisfies the matching criteria, or it will return the address of the data block to permit access of contiguous data. Some memories will simply return a binary bit, indicating whether the input data are present or not present. Because the human brain operates in a neural, associative mode, many computer scientists believe that the development of large capacity, high-speed, associative memories will be required if we are to achieve genuine artificial intelligence. We have implemented the design proposed by Paek and Psaltis (10) by using thin films of bacteriorhodopsin as the photoactive components in holographic associative memories (4). The memory is shown schematically in Fig. 4.

Both the reference and input images are entered into the system using a spatial light modulator (input SLM) and are focused by Fourier lenses (FL) onto the two holographic films, H1 and H2. Fourier association at H1 results in preferential illumination of the pinhole corresponding to the reference image that has the highest correlation (similarity) to the input image, or partial image. The radiation passing through that pinhole illuminates the selected image on H2, which is then transferred out of the associative loop onto a charge-coupled device (CCD) detector. Thresholding is handled electronically, rather than optically, in this implementation. However, optical thresholding can also be done to improve performance (4,10,11). As the example in Fig. 4 shows, only a partial input image is required to generate a complete output image (11).

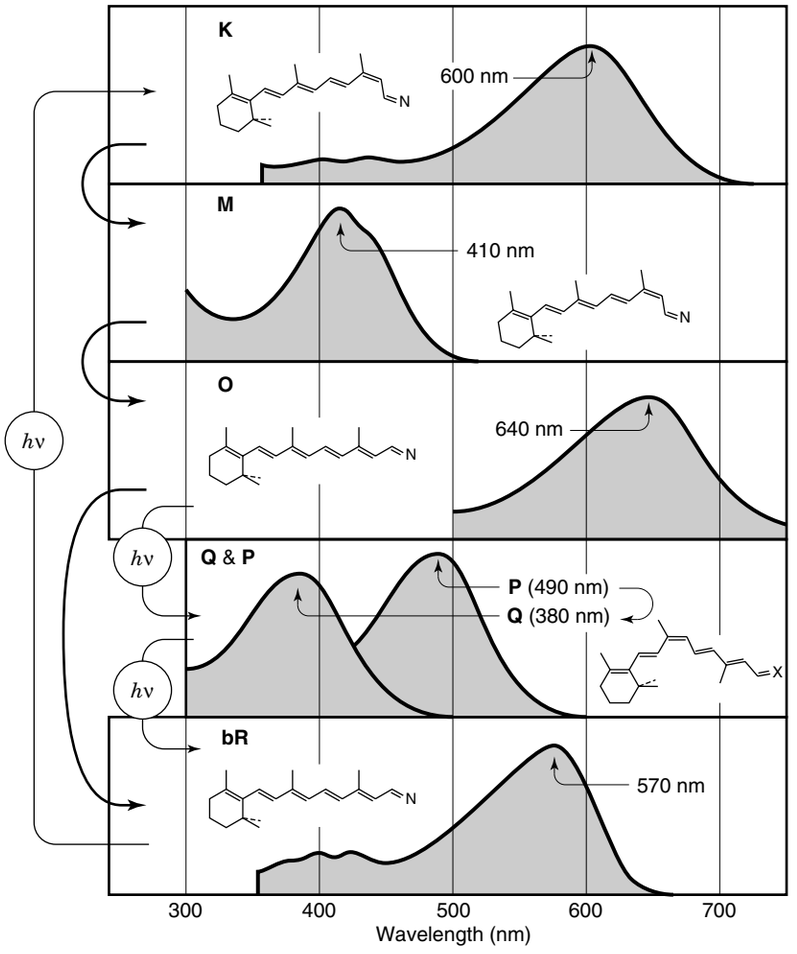

Figure 3. Spectra of select intermediates during the bacteriorhodopsin photocycle. The lighter arrows indicate photochemical transitions, and the solid arrows represent thermal transitions. The insets represent the conformation of the retinal in that state. [N = nitrogen and X = nitrogen in P and oxygen in Q]

The ability to rapidly change the holographic reference patterns from a single optical input, while maintaining both feedback and thresholding, increases the utility of the associative memory; in conjunction with solid-state hardware, the memory can be integrated into hybrid computer architectures. The diffraction limited performance of the protein films, coupled with high write/erase speeds associated with the excellent quantum efficiencies of the these films, represents a key element in the potential of this memory. The ability to modify the protein by selectively replacing one amino acid with another provides significant flexibility in enhancing the properties of the protein (12).

Three-Dimensional Memories

Many scientists believe that the major effect of molecular electronics on computer hardware will be in the area of volumetric memory. There are three different types of protein based volumetric memories currently under investigation: holographic (13–15), simultaneous 2-photon (16–18) and sequential one-photon (9,19). We have already described a holographic memory based on bacteriorhodopsin. Thus, we can focus our discussion on the latter two architectures. These memories read and write information by using two orthogonal laser beams to address an irradiated volume (10 μm^3 to 200 μm^3) within a much larger volume of a photochromic material. Either a simultaneous two-photon or a sequential one-photon process is used to initiate the photochemistry. The former process involves the unusual capability of some molecules to capture two photons simultaneously. The sequential one-photon process requires a material that undergoes a branching reaction, where the first photon activates a cyclical process and the second photon activates a branching reaction to form a stable photoproduct. The 3-dimensional addressing capability of both memories derives from the ability to adjust the location of the irradiated volume in three dimensions. In principle, an optical 3-dimensional memory can store roughly three orders of magnitude more information in the same size enclosure relative to a 2-dimensional optical disk memory. In practice, optical limitations and issues of reliability lower the above ratio to values closer to 300. Nevertheless, a 300-fold improvement in storage capacity is significant. Furthermore, the two-photon or sequential one-photon approach makes parallel addressing of data possible, which enhances data read/write speeds and system bandwidth.

The simultaneous two-photon memory architecture has received a great deal of attention in the past few years, and because bacteriorhodopsin exhibits both high efficiency in capturing two photons and a high yield of producing pho-

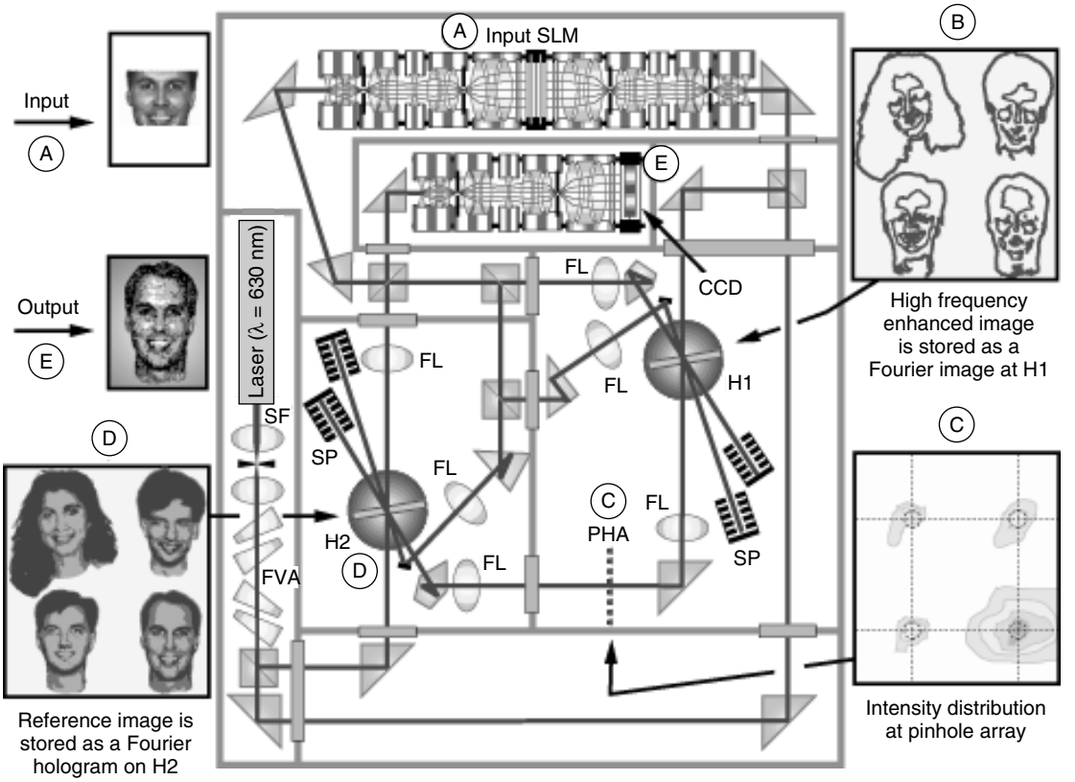

Figure 4. Schematic diagram of a Fourier transform holographic (FTH) associative memory with read/write FTH reference planes using thin polymer films of bacteriorhodopsin to provide real-time storage of the holograms. Note that a partial input image can select and regenerate the entire associated image stored on the reference hologram. Although only four reference images are shown, an optical associative memory can store many hundreds or thousands of images simultaneously. This memory can also work on binary data by using redundant binary representation logic, and a small segment of data can be used to find which page has the largest association with the input segment. Selected components are labeled as follows: FL, Fourier lens; FVA, Fresnel variable attenuator; H1, H2, holographic films; PHA, pin-hole array; SF, spatial filter; SP, beam stop.

toproduct after excitation (20), this material has been a popular memory medium. But more recent studies suggest that the branched-photocycle memory architecture may have greater potential. This sequential one-photon architecture completely eliminates unwanted photochemistry outside of the irradiated volume and provides for a particularly straightforward parallel architecture. We discussed above the use of the **P** and **Q** states for long-term data storage. The fact that these states can only be generated by a temporally separated pulse sequence provides a convenient method of storing data in three dimensions by using orthogonal laser excitation. The process is based on the following sequence: where **K**, **L**, **M**, **N**, and **O** are all intermediates within the main photocycle, and **P** and **Q** are intermediates in the branching cycle (Fig. 5). The numbers underneath the letters give the wavelengths of the absorption maxima of the intermediates in nanometers

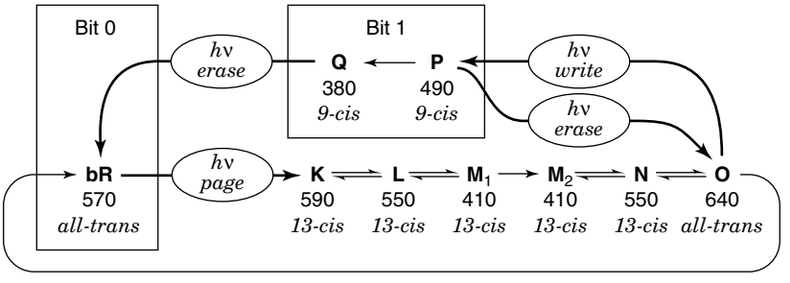

Figure 5. Storing data in three dimensions using orthogonal laser excitation.

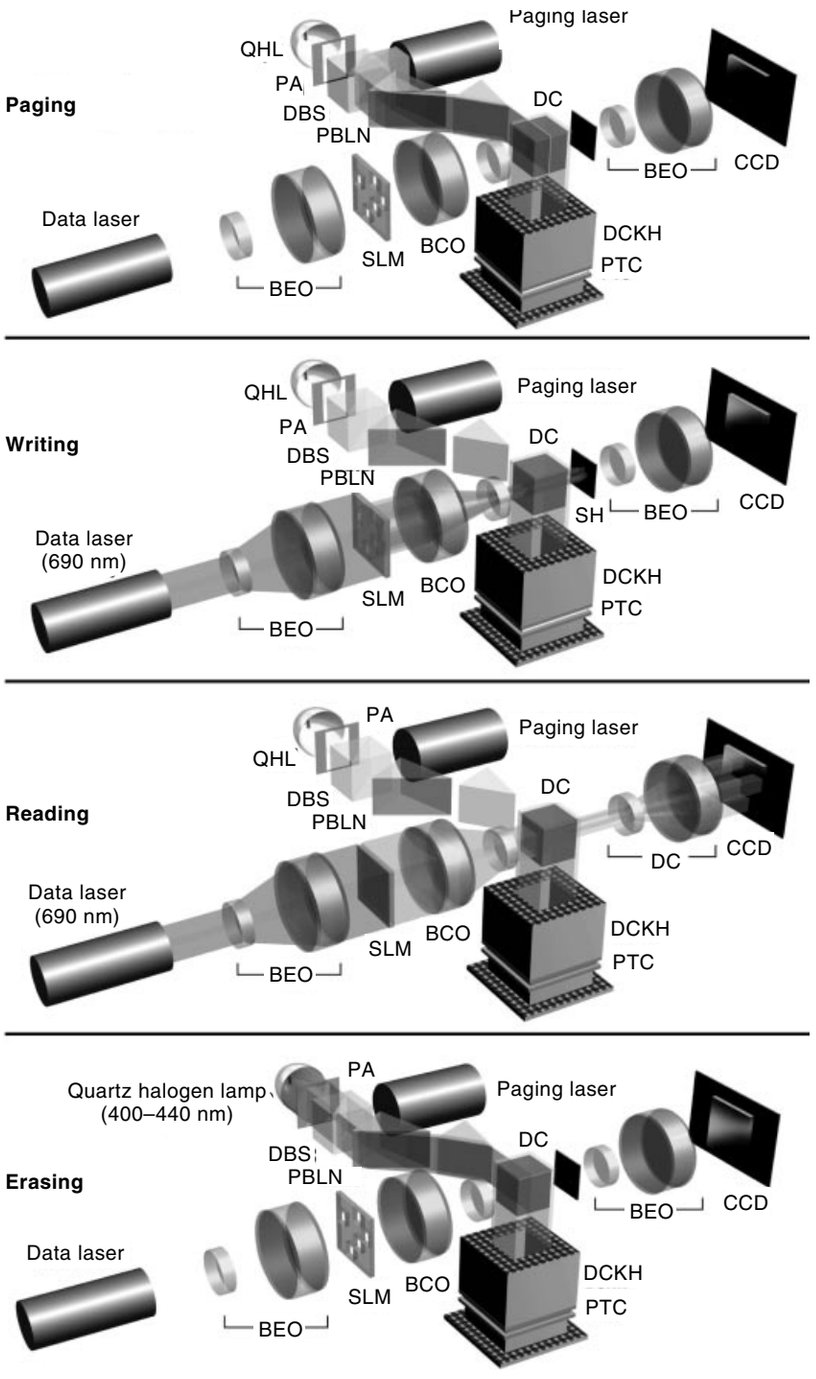

Figure 6. Schematic diagram of the branched-photocycle 3-dimensional memory. The four operations associated with the process of data storage, retrieval, and erasure are shown. Both writing and reading take place within a thin page of material, selected by activating the paging beam. The position of the page is selected by moving the location of the paging beam by using miniature actuators. In the actual system, there are two paging laser systems on both sides of the data cuvette, but we show only one for clarity. Individual components are labeled as follows: QHL, quartz halogen lamp (used for data erase); PA, page aperature; DBS, dichroic beam splitter; BEO, beam expanding optics; SLM, spatial light modulator (selects which data within the page will be written); BCO, beam condensing optics; DC, data cuvette containing the protein in a transparent polymer matrix; CCD, charge coupled device (reads data); DCKH, data cuvette kinematic holder; PTC, Peltier temperature controller.

(for example, **bR** has a maximum absorbance at 570 nm, in the yellow-green region; **O** absorbs at 640 nm, in the red region).

The reading and writing process starts by selecting a very thin region (~15 μm) inside the data cuvette by a process called "paging" (top, Fig. 6). In this process, the paging lasers (there are two, one on each side of the data cuvette, but only one is shown for clarity) with a wavelength in the region 550 nm to 640 nm initiates the photocycle within a ~15 μm slice of the memory medium. The photocycle will return to the resting state (**bR**) in about 10 ms, the time window during which subsequent writing or reading must takes place. In the absence of secondary laser stimulation, the protein within the paged region will simply return to the resting state.

A parallel write is accomplished by using the sequential one-photon optical protocol. The paging beam activates the photocycle of bacteriorhodopsin, and after a few milliseconds the **O** intermediate approaches maximal concentration. The data laser and the SLM are now activated (λ = 680 nm, $\Delta t \approx$ 3 ms) to irradiate those volume elements into which "1" bits

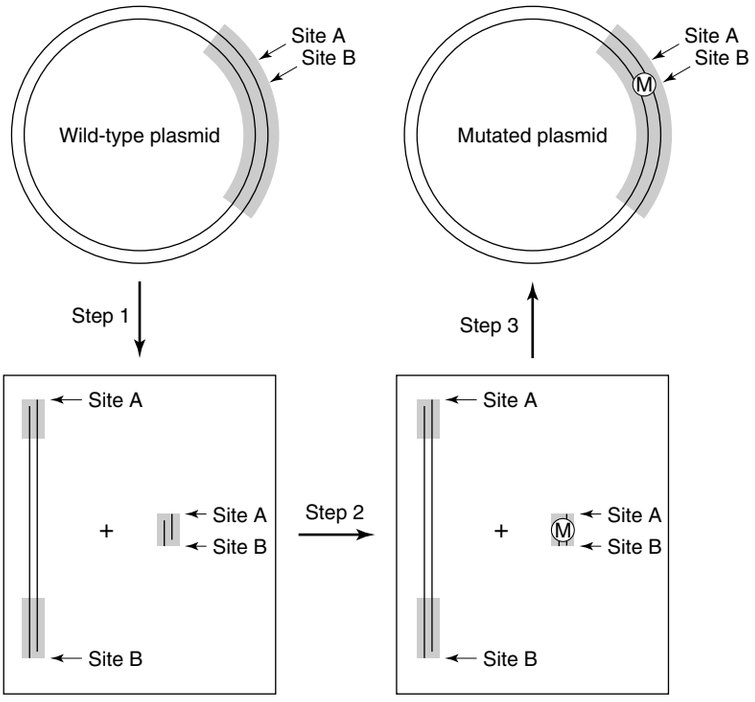

Figure 7. General scheme for cassette mutagenesis. The double circles represent a double-stranded plasmid, and the gray region indicates a gene. Restriction sites unique to the plasmid are on each side the region to be mutated. The distance from site A to site B should not be more than 80 nucleotides. In Step 1, enzymes A and B are added to digest the plasmid at Sites A and B only, producing two linear pieces of DNA. The large fragment is then purified by gel electrophoresis, and added to a synthetic piece of DNA which contains the desired mutation (denoted by a white *M* in a black circle) (Step 2). In the final step (Step 3), the small synthetic fragment containing the desired mutation) is ligated onto the large fragment. One end of the fragment then ligates with the other end to produce a circular mutant plasmid. The plasmid can then be expressed in bacteria to produce protein.

are to be written. This process converts **O** to **P** in these, and only these, locations within the memory cuvette. After many minutes, the **P** state thermally decays to form the **Q** state (the $\mathbf{P} \rightarrow \mathbf{Q}$ decay time, τ_P, is highly dependent upon temperature and polymer matrix). The write process is accomplished in ~10 ms, the time it takes the protein to complete the photocycle.

The read process takes advantage of the fact that light around 680 nm is absorbed by only two intermediates in the photocycle of light-adapted bacteriorhodopsin, the primary photoproduct **K** and the relatively long-lived **O** intermediate (see Fig. 3). The read sequence starts out in a fashion identical to that of the write process by activating the 568 nm paging beam. After two milliseconds, the data timing (DTS) and the data read (DRS) shutters are opened for 1 ms, but the SLM is left off, allowing only 0.1% of the total laser power through. A CCD array (clocked to clear all charges prior to reading) images the light passing through the data cuvette. Those elements in binary state 1 (**P** or **Q**) do not absorb the 680 nm light, but those volumetric elements that started out in the binary 0 state (**bR**) absorb the 680 nm light, because these elements have cycled into the **O** state. Noting that all of the volumetric elements outside of the paged area are restricted to the **bR**, **P**, or **Q** states, the only significant absorption of the beam is associated with **O** states within the paged region. The CCD detector array therefore observes the differential absorptivity of the paged region and the paged region alone. This selectivity is the key to the read operation, and it allows a reasonable signal-to-noise ratio even with thick (1 cm to 1.6 cm) memory media containing $>10^3$ pages. Because the absorptivity of the **O** state within the paged region is more than 1000 times higher than the absorptivity of the remaining volume elements combined, a very weak beam can be used to generate a large differential signal. The read process is complete in ~10 ms, which gives a rate of 10 MB/s. Each read operation must be monitored for each page, and a refresh operation performed after ~1000 reads. While data refresh slows the memory slightly, page caching can minimize the effect.

Data erase is accomplished by using a filtered quartz halogen lamp, the blue light from which photochemically converts both **P** and **Q** back to **bR**. Because this light is not coherent, single-page focusing is not possible, and multiple pages are cleared simultaneously. The optimal wavelength for erasing data is ~410 nm. Alternatively, one can clear an entire data cuvette by using incoherent light in the 360 to 450 nm range. The latter option may prove useful for some less expensive implementations.

Genetic Engineering

Genetic engineering is the systematic manipulation of the genetic code (such as DNA) of an organism to modify the traits of that organism. Material scientists and molecular electronic engineers view genetic engineering primarily as a tool for changing the properties of biological molecules for potential device applications. While genetic engineering has long been a standard technique in the fields of biochemistry, pharmaceuticals, and agriculture, it has only recently become a standard method in bioelectronics. Although a comprehensive review of the techniques and theory of genetic engineering is beyond the scope of this work, a brief discussion is provided below. Our goal is to provide the reader with an appreciation for the basic methods and procedures, as well as the inherent capabilities of this technique.

Deoxyribonucleic acid (DNA) is the molecule that carries the genetic code for all organisms. DNA is a long, double-stranded biopolymer made up of four nucleotides: adenine (A), guanine (G), thiamine (T), and cytosine (C). A region of DNA that encodes for a single protein is called a gene. A gene can

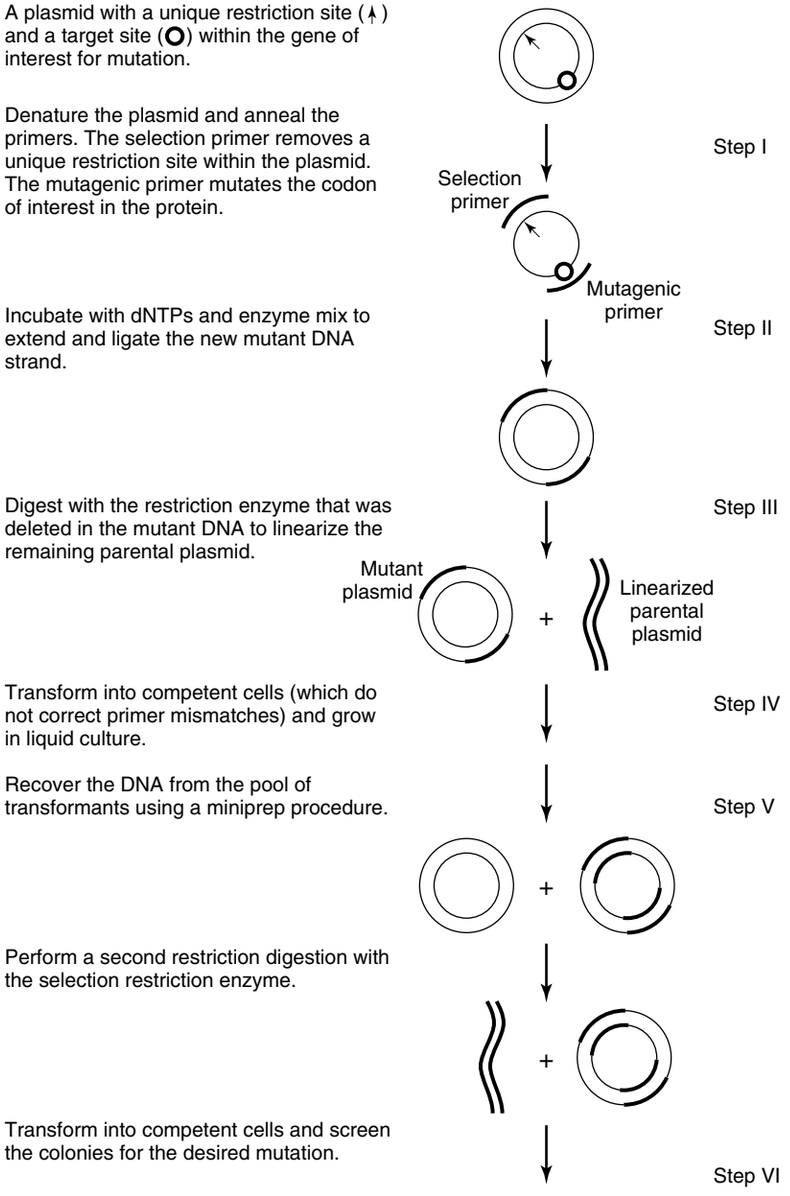

Figure 8. General schematic for mismatched primer mutagenesis. Although Fig. 7 is based on the Chameleon™ Mutagenesis kit (Stratagene, LaJolla, CA), the overall strategy used by this kit is common to all mismatched primer methods. Two simultaneous mutations will be made. One of the mutations will result in a mutant gene (which will produce a mutant protein). The other mutation will silently remove a unique restriction site. Two primers, complementary to the wild-type DNA, are designed with a mutation in each of them. Initially, the DNA is heated to produce single-stranded DNA, and the primers are annealed to the plasmid (Step I). Nucleotides and enzymes extend the primers to form circular DNA (Step II). In Step III, a restriction enzyme cuts only the wild-type DNA. Since a primer silently removed this restriction site in the mutant plasmid, only wild-type DNA is cut. This mixture of DNA is then transformed into *E. coli.* Circular (mutant, in this case) DNA is transformed more efficiently because it is more permeable to the cell membrane (Step IV). The bacteria then amplifies the DNA, and double-stranded mutant and wild-type DNA is isolated (Step V). Another restriction digest linearizes the wild-type DNA, before being transformed. The circular DNA transforms more efficiently, so the mutant DNA is more likely to be transformed. Plasmids are again isolated from the bacteria and sequenced to analyze for the presence of mutants (Step VI).

be isolated and transferred to a circular piece of DNA, called a plasmid, which contains only that gene and the genetic machinery required to express that gene. The average protein is 400 amino acids long, and the average gene is 1200 nucleotides long (21). This relationship occurs because three consecutive nucleotides make a codon, and each codon is ultimately translated to a single amino acid. More than one codon exists for most amino acids. For example, GGG codes for a glycine amino acid, but so do GGT, GGC, and GGA. The amino acids are then constructed in the order of the codons on the DNA. There are 20 different amino acids that are used to make proteins.

A mutation occurs when an amino acid other than that which is present in the native protein is selected by the genetic code. Mutations can take the form of site specific or random replacements, additions of new amino acids, or deletions of amino acids within the primary structure. For a review of mutagenesis see Refs. 22–24. Biochemists and biophysicists routinely use site-specific mutations to study structure-function relationships existing in different proteins. Two strategies most commonly used to construct site-specific mutants are known as cassette and mismatched primer mutagenesis.

Restriction enzymes will cut DNA only at sites within a specific sequence. To perform cassette mutagenesis, the location of the desired mutant must be flanked by two restriction sites unique to the plasmid, and the distance between the two restriction sites must be not more than 80 nucleotides. The sites must be unique in the plasmid because the DNA should be cut into no more than two pieces, a large fragment and a small fragment (Fig. 7). The synthetic fragments are limited to a length of about 80 nucleotides because this is the practical length limit of oligomeric synthesis. Once the small frag-

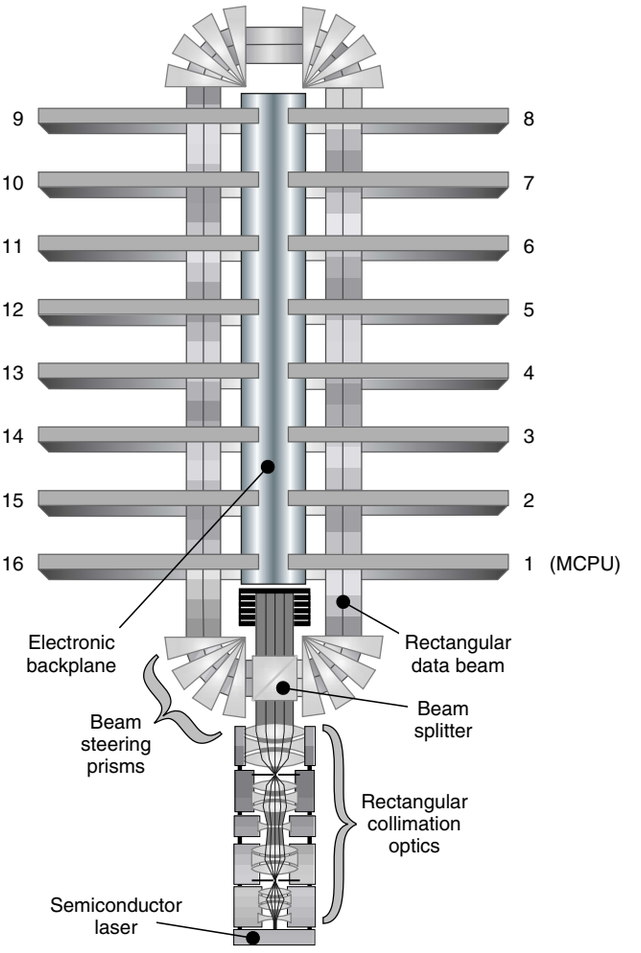

Figure 9. A schematic diagram of the optical data path of the hybrid computer. A semiconductor laser is manipulated by a set of lenses and aperatures to form a homogeneous collimated rectangular or square laser beam. This beam is directed through each of the optical interconnects of the 16 cards and circulates from Card 1 (the main central processing unit or MCPU) through to card 16 and back to Card 1. Each optical interconnect contains an optical read capable spatial light modulator (RCSLM) array of 264 $\times$ 264 elements (see Fig. 10). The beam splitter adds photons from the laser to maintain intensity, but any information transferred onto the optical data path can still be read by the MCPU after one pass through the beam splitter. Each card has a separate optical address and can read data in parallel from the optical data path and, if addressed by the MCPU, can read data from or transfer data onto the 256 $\times$ 256 portion of the array assigned to the data page. The remaining elements are for addressing and error correction. The optical interconnect can transfer data in parallel pages of 8 kbytes, with rates of approximately 24 Mbytes per second. An electronic backplane also connects the cards to provide power and slower electronic data transfer.

ment is removed, a new synthetic oligonucleotide with the desired mutant is attached into place with an enzyme (ligase). Interestingly, one of the first examples of cassette mutagenesis was one by H. Gobind Khorana and co-workers on the bacteriorhodopsin gene (25).

This type of mutagenesis is not always possible because unique restriction sites do not always flank a desired mutation location. If many mutations are going to be performed on a gene, a synthetic gene can be made. A synthetic gene is one where restriction sites are added or deleted until there is a unique restriction site approximately every 70 nucleotides throughout the gene. This is accomplished by using silent mutations, that is mutations that change the DNA sequence but leave the translated amino acid sequence unchanged. This is possible because there are multiple codons for each amino acid (26).

An alternative mutagenesis strategy uses a mismatched primer extension (Fig. 8). This strategy is more common than the cassette method, because it can be used on any sequence. Many different techniques (and many commercially available kits) have been developed to take advantage of the flexibility of this method. This alternative strategy is based on the fact that double-stranded DNA can be denatured and renatured as a function of temperature. A primer containing the desired mutant is added to the denatured DNA, which is single stranded. The primer is designed so that it will be the complement of the wild type DNA, except for the mutation introduced. The DNA is then cooled so that the primer will anneal to the wild type DNA. The primer is then elongated with polymerase enzyme, which makes the complement DNA of the template. Now two strands of DNA exist, the original (template DNA) and the new mutant extended primer. The template DNA is selectively digested (discarded), and the DNA is then replicated (usually using a bacterium like *Escherichia coli*). The resultant mutant DNA is then expressed to obtain the mutant protein.

Genetic engineering has been used to create bacteriorhodopsin mutants with enhanced materials properties (27–31). For example, some mutants have enhanced the holographic properties of the protein by producing an **M** state with an extended lifetime (27–30), while others improve the branched-photocycle memory by enhancing the yield of the **O** state (31). The challenge for material scientists is to predict a priori what amino acid sequence will create or enhance a specific protein property. At present, the vast majority of genetic engineering for materials applications is a trial and error process, due to the complexity of protein structure and function and the lack of satisfactory molecular modeling tools. It is

hoped that continued theoretical work will yield computer programs with the predictive capabilities comparable to the SPICE packages that are the cornerstone of electrical engineering. In this regard, bioelectronics is many years if not decades behind computer engineering.

HYBRID COMPUTERS

The previous discussion has emphasized the internal architectures of two types of optical systems based on bacteriorhodopsin. The first step in the evolutionary development of computers will be the generation of hybrid systems that combine some of the best features of semiconductor, optical, and molecular architectures. It is well known that current semiconductor computers are limited not so much by processor speed as by interconnect speeds and memory capacity. During the past decade, the speed of computer processors has increased between two and three orders of magnitude. This dramatic increase in processor capability has been unmatched by a corresponding increase in data storage densities, which have increased by only one order of magnitude in both random access memory and hard disk technology. Of equal importance is the recognition that transferring data within the computer is the principal bottleneck that limits performance. Optical architectures provide for the transfer of massive amounts of data in parallel, and hybrid computers may take advantage of this capability by using optical interconnects to access a beam of coherent light that passes through each card (Fig. 9). Each card will be capable of reading data from the beam and writing data onto the beam by using a square or rectangular array of independently addressable pixels, which sense light (by using thin film photovoltaic materials such as bacteriorhodopsin) and interrupt light (by using liquid crystal or ferroelectric molecules) (Fig. 10). Our proposed system uses an optical read/write array of 264×264 elements with a 256×256 portion of the array assigned to the data page. The remaining elements are for addressing and error correction. This device is called a Read Capable Spatial Light Modulator (RCSLM) and represents one of many possible designs for optical interconnects. The key feature of this design is that any card along the optical path can take over control of the data portion and all cards along the optical path can read data simultaneously. Although each RCSLM extracts a small amount of light from the data beam, by using thin film technology, the attenuation per card is small and as many as 32 cards can share the same optical path before optical repeaters are required. A key advantage of this type of optical interconnect is that it can be made inexpensively (projected costs of less than $100 per unit). A single main central processor (MCPU) mediates all of the activity, but the power of the computer derives from the distributed processing capability inherent in the hybrid architecture. Four sample cards, three of which use the protein based architectures discussed in this chapter, are shown in Fig. 10. Nevertheless, the use of a semiconductor MCPU emphasizes the hybrid character of the computer.

The type of hybrid computer envisioned here would be highly flexible, and by selecting the appropriate cards, could be designed to handle large database problems, complex scientific simulations, or serve as a unique platform for investigations of artificial intelligence. By providing close to a terabyte (10^9 bytes) of paged memory, this computer can handle large scientific and numerical data bases with alacrity. The availability of optical associative processing, coupled with paged volumetric memory, will make database searches many orders of magnitude faster than currently possible; it will provide a unique platform for investigating the importance and capabilities of massive associative processing in artificial intelligence. Because this hybrid computer can be designed to function as a neural associative computer capable of both binary and image association and learning, the potential importance of hybrid computers to studies in artificial intelligence cannot be underestimated.

We close by emphasizing that the hybrid computer described here does not yet exist. While such speculation is based on a solid foundation of fundamental research, further

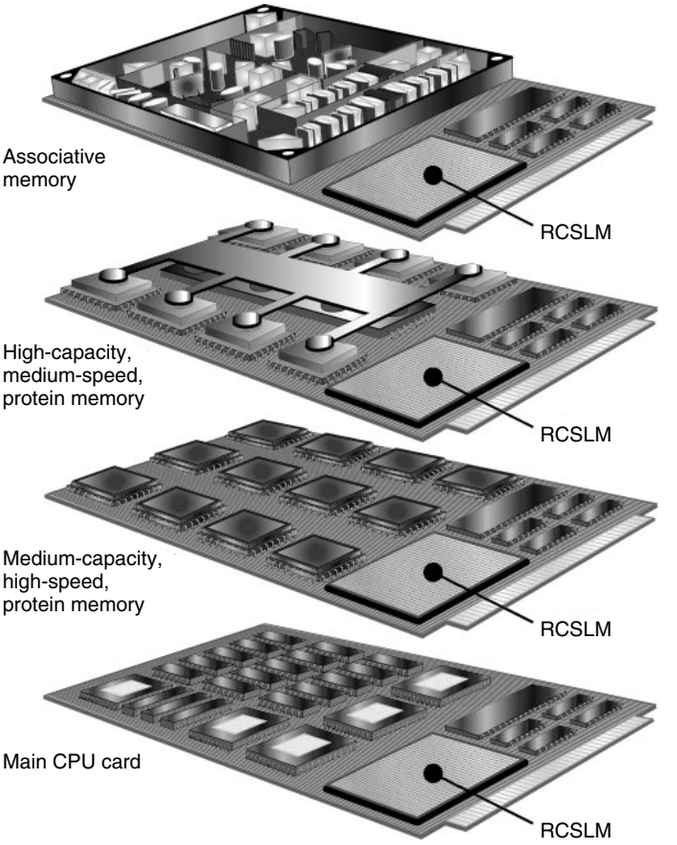

Figure 10. Four examples of potential cards for use in the hybrid computer. All cards share a common 264×264 element RCSLM. The first card (bottom) is the main central processing unit (MCPU) based on a semiconductor based, reduced instruction set (RISC) processor. The second card is a protein based, branched-photocycle, volumetric memory capable of storing 32 GBytes of data. The third card is an 8 GByte volumetric memory, which uses slower, actuator-based paging, but provides removable storage. This latter card is comparable to current magnetic disk storage in speed, but provides comparable density with removable media. The fourth card (top) is a paged, optical associative memory capable of handling either image or block redundant binary data. Molecular electronics contributes to the architecture of the cards by providing the ferroelectric SLM, the protein-based volumetric memory elements, and the thin film holographic media for the associative memory.

developmental work will be necessary to create such a computer. Other competing architectures are also under study, and it is likely that many of the hardware components described here will be replaced with alternative architectures in the course of developing a powerful yet cost-effective design. Nevertheless, we can be confident that hybrid computers will be available at various stages of implementation within the next five years, and that they will evolve into the dominant architectures for some types of computing during the next two decades. The extent to which hybrid computers will affect personal computing remains an open question, but we anticipate that molecular based volumetric memories will ultimately find application at all levels of computing, from personal computers to large supercomputers.

BIBLIOGRAPHY

1. R. R. Birge, A. F. Lawrence, and J. A. Tallent, Quantum effects, thermal statistics and reliability of nanoscale molecular and semiconductor devices, *Nanotechnology* **2**: 73–87, 1991.
2. R. W. Keyes, Electronic devices in large systems, *AIP Conf. Proc.,* **262**: 285–297, 1992.
3. R. R. Birge, Introduction to molecular and biomolecular electronics, *Adv. Chem.,* **240**: 1–14, 1994.
4. R. R. Birge et al., Protein-based three-dimensional memories and associative processors, in M. A. Ratner and J. Jortner (eds.), *Molecular Electronics*, Oxford, U.K.: Blackwell Science, pp. 439–471, 1997.
5. E. R. Kandel, J. H. Schwartz, and T. Jessell, *Principles of Neural Science,* 3rd ed., Norwalk, CT, Appleton & Lange, 1991.
6. M. Reed and A. C. Seabaugh, Prospects for semiconductor quantum devices, *Adv. Chem.,* **240**: 15–42, 1994.
7. R. R. Birge, Molecular and biomolecular electronics, *Adv. Chem.,* **240**: 596, 1994.
8. M. A. Ratner and J. Jortner, *Molecular Electronics,* Oxford: Blackwell Science, 1997.
9. R. R. Birge et al., Bioelectronics, three-dimensional memories and hybrid computers, *IEEE IEDM Tech. Dig.,* **94**: 3–6, 1994.
10. E. G. Paek and D. Psaltis, Optical associative memory using Fourier transform holograms, *Opt. Eng.,* **26**: 428–433, 1987.
11. R. B. Gross, K. C. Izgi, and R. R. Birge, Holographic thin films, spatial light modulators and optical associative memories based on bacteriorhodopsin, *Proc. SPIE,* **1662**: 186–196, 1992.
12. N. Hampp et al., Bacteriorhodopsin variants for holographic pattern recognition, *Adv. Chem.,* **240**: 511–526, 1994.
13. L. d'Auria et al., Experimental holographic read-write memory using 3-D storage, *Appl. Opt.,* **13**: 808–818, 1974.
14. R. R. Birge, Photophysics and molecular electronic applications of the rhodopsins, *Annu. Rev. Phys. Chem.,* **41**: 683–733, 1990.
15. J. F. Heanue, M. C. Bashaw, and L. Hesselink, Volume holographic storage and retrieval of digital data, *Science,* **265**: 749–752, 1994.
16. D. A. Parthenopoulos and P. M. Rentzepis, Three-dimensional optical storage memory, *Science,* **245**: 843–845, 1989.
17. Z. Chen et al., Advances in protein-based three-dimensional optical memories, *BioSystems,* **35**: 145–151, 1995.
18. A. S. Dvornikov and P. M. Rentzepis, 3D Optical Memory Devices. System and Materials Characteristics, *Proc. IEEE Nonvol. Mem. Tech. (INVMTC),* 1996, pp. 40–44.
19. J. A. Stuart et al., Protein-based volumetric memory, *Proc. IEEE Nonvol. Mem. Tech. (INVMTC),* **6**: 45–51, 1996.
20. R. R. Birge and C. F. Zhang, Two-photon spectroscopy of light-adapted bacteriorhodopsin, *J. Chem. Phys.,* **92**: 7178–7195, 1990.
21. J. D. Watson et al., *Recombinant DNA,* 2nd ed., New York: Scientific American Books, 1992, pp. 42–43.
22. D. Botstein and D. Shortle, Strategies and applications of in vitro mutagenesis, *Science,* **229**: 1193–1201, 1985.
23. M. Smith, In vitro mutagenesis, in A. Campbell (ed.), *Annual Review of Genetics* **19**: Palo Alto, CA: Annual Reviews Inc., pp. 423–462, 1985.
24. J. F. Reidhaar-Olson and R. T. Sauer, Combinatorial cassette mutagenesis as a probe of the informational content of protein sequences, *Science,* **241**: 53–57, 1988.
25. K. M. Lo et al., Specific amino acid substitutions in bacterioopsin: Replacement of a restriction fragment in the structural gene by synthetic DNA fragments containing altered codons, *Proc. Natl. Acad. Sci. USA,* **81**: 2285–2289, 1984.
26. L. Ferretti et al., Total synthesis of a gene for bovine rhodopsin, *Proc. Natl. Acad. Sci. USA,* **83**: 599–603, 1986.
27. C. Gergely et al., Study of the photocycle and charge motions of the bacteriorhodopsin mutant D96N, *Biophys. J.,* **65**: 2478–2483, 1993.
28. L. J. W. Miercke et al., Wild-type and mutant bacteriorhodopsins D85N, D96N, and R82Q: Purification to homogeneity, pH dependence of pumping and electron diffraction, *Biochemistry,* **30**: 3088–3098, 1991.
29. N. Hampp et al., Diffraction efficiency of bacteriorhodopsin films for holography containing bacteriorhodopsin wild-type BRwt and its variants BR_{D85E} and BR_{D96N}, *J. Phys. Chem.,* **96**: 4679–4685, 1992.
30. D. Zeisel and N. Hampp, Spectral relationship of light-induced refractive index and absorption changes in bacteriorhodopsin films containing wild-type BR_{wt} and the variant BR_{D96N}, *J. Phys. Chem.,* **96**: 7788–7792, 1992.
31. S. Misra et al., Proton uptake and release are rate-limiting steps in the photocycle of the bacteriorhodopsin mutant E204Q, *Biochemistry,* **36**: 4875–4883, 1997.

BRYAN W. VOUGHT
ROBERT R. BIRGE
Syracuse University

MONITORING. See FAULT DIAGNOSIS.

MONITORING, PATIENT. See PATIENT MONITORING.